

A New Route to the Synthesis of Phosphine-Substituted Diiron Aza- and Oxadithiolate Complexes

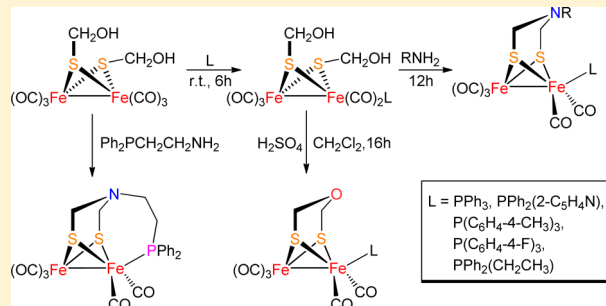
Jiao He,[†] Cheng-Long Deng,[†] Yao Li,[†] Yu-Long Li,^{*,†} Yu Wu,[†] Li-Ke Zou,[†] Chao Mu,[†] Qiang Luo,[†] Bin Xie,[†] Jian Wei,[†] Jing-Wen Hu,[†] Pei-Hua Zhao,^{*,‡} and Wen Zheng[†]

[†]College of Chemistry and Environmental Engineering, Sichuan University of Science & Engineering, Zigong 643000, P. R. China

[‡]School of Materials Science and Engineering, North University of China, Taiyuan 030051, P. R. China

Supporting Information

ABSTRACT: Diiron dithiolate complexes have received special attention because of their structural similarity to the active site of [FeFe]-hydrogenases, which are the most efficient and fastest catalysts for the generation of dihydrogen in nature. Recently, we established a novel and efficient way to prepare phosphine-substituted diiron aza- and oxadithiolate complexes. Reaction of $\text{Fe}_2(\mu\text{-SCH}_2\text{OH})_2(\text{CO})_6$ and several phosphine ligands L (L = PPh_3 , $\text{PPh}_2(2\text{-C}_5\text{H}_4\text{N})$, $\text{P}(\text{C}_6\text{H}_4\text{-4-CH}_3)_3$) affords the intermediate $\text{Fe}_2(\mu\text{-SCH}_2\text{OH})_2(\text{CO})_5\text{L}$, while the intermediate *in situ* reacts with primary amines RNH_2 (R = $\text{CH}_2\text{CH}_2\text{CH}(\text{CH}_3)_2$, $\text{CH}_2\text{CH}_2\text{CH}_2\text{SCH}_3$, $\text{C}_6\text{H}_4\text{-4-CH}_3$) to produce the target phosphine-substituted diiron azadithiolate complexes $\text{Fe}_2[(\mu\text{-SCH}_2)_2\text{NCH}_2\text{CH}_2\text{CH}(\text{CH}_3)_2](\text{CO})_5(\text{PPh}_3)$ (**1**), $\text{Fe}_2[(\mu\text{-SCH}_2)_2\text{NCH}_2\text{CH}_2\text{CH}(\text{CH}_3)_2](\text{CO})_5[\text{PPh}_2(2\text{-C}_5\text{H}_4\text{N})]$ (**2**), $\text{Fe}_2[(\mu\text{-SCH}_2)_2\text{NCH}_2\text{CH}_2\text{CH}(\text{CH}_3)_2](\text{CO})_5[\text{P}(\text{C}_6\text{H}_4\text{-4-CH}_3)_3]$ (**3**), $\text{Fe}_2[(\mu\text{-SCH}_2)_2\text{NCH}_2\text{CH}_2\text{CH}_2\text{SCH}_3](\text{CO})_5(\text{PPh}_3)$ (**4**), $\text{Fe}_2[(\mu\text{-SCH}_2)_2\text{NCH}_2\text{CH}_2\text{CH}_2\text{SCH}_3](\text{CO})_5[\text{PPh}_2(2\text{-C}_5\text{H}_4\text{N})]$ (**5**), $\text{Fe}_2[(\mu\text{-SCH}_2)_2\text{NCH}_2\text{CH}_2\text{CH}_2\text{SCH}_3](\text{CO})_5[\text{P}(\text{C}_6\text{H}_4\text{-4-CH}_3)_3]$ (**6**), $\text{Fe}_2[(\mu\text{-SCH}_2)_2\text{N C}_6\text{H}_4\text{-4-CH}_3](\text{CO})_5[\text{PPh}_2(2\text{-C}_5\text{H}_4\text{N})]$ (**7**), and $\text{Fe}_2[(\mu\text{-SCH}_2)_2\text{N C}_6\text{H}_4\text{-4-CH}_3](\text{CO})_5[\text{P}(\text{C}_6\text{H}_4\text{-4-CH}_3)_3]$ (**8**) in moderate yields. A novel complex $\text{Fe}_2[(\mu\text{-SCH}_2)_2\text{NCH}_2\text{CH}_2\text{PPh}_2](\text{CO})_5$ (**9**) can be obtained by reaction of $\text{Fe}_2(\mu\text{-SCH}_2\text{OH})_2(\text{CO})_6$ and $\text{Ph}_2\text{PCH}_2\text{CH}_2\text{NH}_2$. In addition, according to the same strategy, phosphine-substituted diiron oxadithiolate complexes $\text{Fe}_2[(\mu\text{-SCH}_2)_2\text{O}](\text{CO})_5[\text{P}(\text{C}_6\text{H}_4\text{-4-F})_3]$ (**10**), $\text{Fe}_2[(\mu\text{-SCH}_2)_2\text{O}](\text{CO})_5[\text{P}(\text{C}_6\text{H}_4\text{-4-CH}_3)_3]$ (**11**), and $\text{Fe}_2[(\mu\text{-SCH}_2)_2\text{O}](\text{CO})_5(\text{Ph}_2\text{PCH}_2\text{CH}_3)$ (**12**) have been successfully synthesized. All of the new complexes **1–12** were fully characterized by elemental analysis, IR, and NMR spectroscopy, and particularly for **1–4**, **6**, **7**, and **9–11** by X-ray single diffraction analysis. Moreover, complexes **1** and **10** were found to be catalysts for H_2 production under electrochemical conditions.



INTRODUCTION

In recent years, diiron dithiolate complexes have received special attention because of their structural similarity to the active site of [FeFe]-hydrogenases, which are the most efficient and fastest catalysts for the generation of dihydrogen in nature.^{1–5} The study of the structure and functionality of the active site of the [FeFe]-hydrogenases is significant, since it is helpful for the design and synthesis of new low-cost and efficient catalysts for H_2 production and a pathway for solving the problem of energy crisis.⁶ Crystallographic analyses of the [FeFe]-hydrogenase enzymes were reported by Peters as well as Fontecilla-Camps et al., demonstrating that the active site of [FeFe]-hydrogenases consists of a butterfly [2Fe2S] cluster linked to a cubane-like [4Fe4S] cluster through a cysteine bridge (Figure 1).^{7–13} The Fe atoms of the [2Fe2S] cluster are coordinated by CO and CN^- ligands, as shown by FTIR spectroscopy studies;⁷ meanwhile, the bridging dithiolate unit is proposed to be $\text{SCH}_2\text{XCH}_2\text{S}$ (X = CH_2 , NH, O).^{8–12} It is generally accepted that the [2Fe2S] cluster is the catalytic

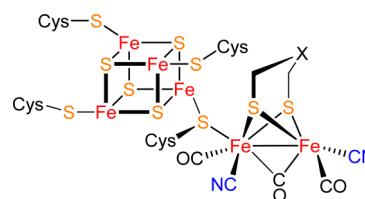


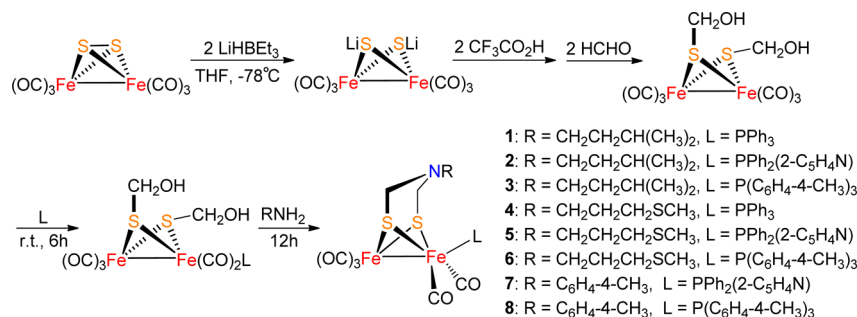
Figure 1. Active site structure of [FeFe] hydrogenase (X = CH_2 , NH, O).

center,¹³ resulting in the synthesis of the diiron dithiolate carbonyl complexes.

Rauchfuss and co-workers first prepared the parent azadithiolate $\text{Fe}_2[(\mu\text{-SCH}_2)_2\text{NH}](\text{CO})_6$ by treatment of $\text{Fe}_2(\mu\text{-SH})_2(\text{CO})_6$ with a mixture of paraformaldehyde and $(\text{NH}_4)_2\text{CO}_3$.¹⁰ Afterward, the azadithiolate complexes of the type $\text{Fe}_2[(\mu\text{-SCH}_2)_2\text{NR}](\text{CO})_6$ can be prepared by the

Received: January 17, 2017

Scheme 1. Synthesis of the Phosphine-Substituted Diiron Azadithiolate Complexes 1–8 via One-Pot Reaction



alkylation of Fe₂(μ-SLi)₂(CO)₆ using (ClCH₂)₂NR or the reaction of Fe₂(μ-SH)₂(CO)₆ with formaldehyde in the presence of amines.^{14–25} Following these earlier studies, the investigation on the modification of the bridge head group or substitution of carbonyl ligands with Lewis bases have been under intense scrutiny.²⁶ These Lewis bases include phosphines, cyanide, N-heterocyclic carbenes, thioethers, and others.^{27–32} Notably, in the chemistry of preparation of phosphine-substituted diiron azadithiolate complexes, usually the first key step is to synthesize the diiron azadithiolate complexes Fe₂[(μ-SCH₂)₂NR](CO)₆, then the second step is to replace the CO ligand by a phosphine ligand in the presence of a decarbonylation agent Me₃NO, refluxing, or photolysis.^{33–35} Although the aforementioned method has been widely used, such a traditional route is complicated.

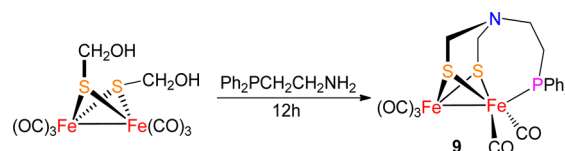
Recently, we have successfully established a novel and efficient way to prepare phosphine-substituted diiron azadithiolate complexes.^{14,36} Inspired by the new finds and in continuation of our research on [FeFe]-hydrogenase model complexes, our strategy is to prepare this kind of the phosphine-substituted diiron azadithiolate complexes by reaction of Fe₂(μ-SCH₂OH)₂(CO)₆ and phosphine ligand, followed by addition of amine. According to the above one-pot reaction, a series of new phosphine-substituted diiron azadithiolate complexes have been successfully synthesized in satisfactory yield. In addition, according to the same strategy, phosphine-substituted diiron oxadithiolate complexes have also been prepared via reaction of Fe₂(μ-SCH₂OH)₂(CO)₆ and phosphine ligands, followed by treatment with H₂SO₄. The electrochemical properties of these diiron aza- and oxadithiolate complexes were studied by cyclic voltammetry (CV), some of which were further found to be catalysts for H₂ production under electrochemical conditions. Herein, we report the synthesis, structural characterization, and electrochemical properties of 12 new diiron aza- and oxadithiolate complexes containing different phosphine ligands.

RESULTS AND DISCUSSION

In order to explore a simple and high efficient way to synthesize the phosphine-substituted diiron dithiolate complexes, new complexes 1–8 were prepared as shown in Scheme 1. Treatment of Fe₂(μ-SCH₂OH)₂(CO)₆ with several phosphine ligands L (L = PPh₃, PPh₂(2-C₅H₄N), P(C₆H₄-4-CH₃)₃) affords the intermediate Fe₂(μ-SCH₂OH)₂(CO)₅L, followed by the *in situ* addition of amines RNH₂ (R = CH₂CH₂CH(CH₃)₂, CH₂CH₂CH₂SCH₃, C₆H₄-4-CH₃) to produce the target complexes Fe₂[(μ-SCH₂)₂NCH₂CH₂CH(CH₃)₂](CO)₅(PPh₃) (1), Fe₂[(μ-SCH₂)₂NCH₂CH₂CH(CH₃)₂](CO)₅[PPh₂(2-C₅H₄N)] (2), Fe₂[(μ-SCH₂)₂NCH₂CH₂CH-

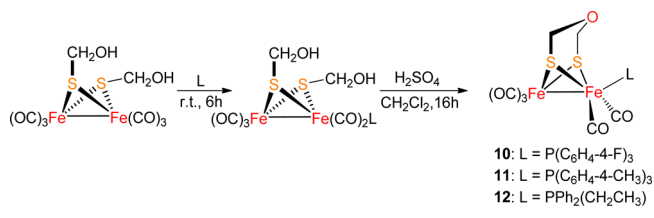
(CH₃)₂](CO)₅[P(C₆H₄-4-CH₃)₃] (3), Fe₂[(μ-SCH₂)₂NCH₂CH₂CH₂SCH₃](CO)₅(PPh₃) (4), Fe₂[(μ-SCH₂)₂NCH₂CH₂CH₂SCH₃](CO)₅[PPh₂(2-C₅H₄N)] (5), Fe₂[(μ-SCH₂)₂NCH₂CH₂CH₂SCH₃](CO)₅[P(C₆H₄-4-CH₃)₃] (6), Fe₂[(μ-SCH₂)₂NC₆H₄-4-CH₃](CO)₅[PPh₂(2-C₅H₄N)] (7), and Fe₂[(μ-SCH₂)₂NC₆H₄-4-CH₃](CO)₅[P(C₆H₄-4-CH₃)₃] (8) in moderate yields. In addition, according to Scheme 2, reaction of Fe₂(μ-SCH₂OH)₂(CO)₆ and

Scheme 2. Synthesis of the Phosphine-Substituted Diiron Azadithiolate Complex 9



Ph₂PCH₂CH₂NH₂ affords a novel phosphine-substituted diiron azadithiolate complex Fe₂[(μ-SCH₂)₂NCH₂CH₂PPh₂](CO)₅ (9). Furthermore, according to Scheme 3, reaction of Fe₂(μ-

Scheme 3. Synthesis of the Phosphine-Substituted Diiron Oxadithiolate Complexes 10–12



SCH₂OH)₂(CO)₅L (L = P(C₆H₄-4-F)₃, P(C₆H₄-4-CH₃)₃, and Ph₂PCH₂CH₃) with H₂SO₄ in CH₂Cl₂ produces phosphine-substituted diiron oxadithiolate complexes Fe₂[(μ-SCH₂)₂O](CO)₅[P(C₆H₄-4-F)₃] (10), Fe₂[(μ-SCH₂)₂O](CO)₅[P(C₆H₄-4-CH₃)₃] (11), and Fe₂[(μ-SCH₂)₂O](CO)₅[PPh₂(CH₂CH₃)] (12). It is worthy to note that compared with the traditional way to prepare diiron dithiolate complexes containing phosphine ligands, our one-pot reaction is simpler and more efficient. For example, as shown in Table 1, complexes 1–8 can be obtained in 31–57% yields using our one-pot reaction (Method A). Comparatively, we tried to synthesize complexes 1–8 by two-step reactions (Method B) in the followings: (i) the reaction of Fe₂(μ-SCH₂OH)₂(CO)₆ and RNH₂ (R = CH₂CH₂CH(CH₃)₂, CH₂CH₂CH₂SCH₃, C₆H₄-4-CH₃) to obtain the purified complex Fe₂[(μ-SCH₂)₂NR](CO)₆; and (ii) the treatment of the as-prepared Fe₂[(μ-SCH₂)₂NR](CO)₆ with L (L = PPh₃, PPh₂(2-C₅H₄N), P(C₆H₄-4-CH₃)₃) in the

Table 1. Yields of Complexes 1–8 Derived From $\text{Fe}_2(\mu\text{-SCH}_2\text{OH})_2(\text{CO})_6$ by Methods A and B

complex	Method A: $\text{Fe}_2(\mu\text{-SCH}_2\text{OH})_2(\text{CO})_5\text{L} + \text{RNH}_2$ (yield)	Method B: $\text{Fe}_2(\mu\text{-SCH}_2\text{OH})_2(\text{CO})_6 + \text{RNH}_2 + \text{Me}_3\text{NO} + \text{L}$ (yield)
1	56%	23%
2	43%	21%
3	51%	24%
4	42%	20%
5	45%	20%
6	41%	19%
7	31%	16%
8	33%	17%

presence of decarbonylating agent Me_3NO to afford the target complexes 1–8 in low yields (16–24%, calculated by $\text{Fe}_2(\mu\text{-S})_2(\text{CO})_6$). Moreover, the intermediate $\text{Fe}_2(\mu\text{-SCH}_2\text{OH})_2(\text{CO})_5(\text{PPh}_3)$, which was monitored by IR spectroscopy, displays three absorption bands in the region 1928–2041 cm^{-1} for $\nu_{\text{C}\equiv\text{O}}$. This observation is consistent with those observed in the coordination of phosphine ligand PPh_3 to the Fe core of the diiron carbonyl complexes.²⁸

Complexes 1–12 have been fully characterized by elemental analysis, IR, ^1H NMR, ^{13}C NMR, and ^{31}P NMR spectroscopy. The IR spectra of complexes 1–12 display three or four strong absorption bands in the range of 1924–2052 cm^{-1} for their terminal carbonyls (Table 2), which are shifted toward lower

Table 2. IR Data of the Carbonyl Stretching Frequencies for Complexes 1–12

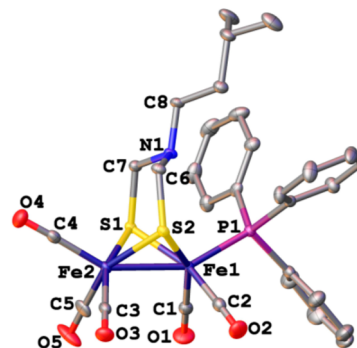
complex	$\nu_{\text{C}\equiv\text{O}}$ (KBr disk, cm^{-1})
$\text{Fe}_2[(\mu\text{-SCH}_2)_2\text{NCH}_2\text{CH}_2\text{CH}(\text{CH}_3)_2](\text{CO})_5(\text{PPh}_3)$	2040/1984/1976/1932
$\text{Fe}_2[(\mu\text{-SCH}_2)_2\text{NCH}_2\text{CH}_2\text{CH}(\text{CH}_3)_2](\text{CO})_5[\text{PPh}_2(2\text{-C}_5\text{H}_4\text{N})]$	2038/1987/1970/1955
$\text{Fe}_2[(\mu\text{-SCH}_2)_2\text{NCH}_2\text{CH}_2\text{CH}(\text{CH}_3)_2](\text{CO})_5[\text{P}(\text{C}_6\text{H}_4\text{-4-CH}_3)_3]$	2038/1988/1969/1955
$\text{Fe}_2[(\mu\text{-SCH}_2)_2\text{NCH}_2\text{CH}_2\text{CH}_2\text{SCH}_3](\text{CO})_5(\text{PPh}_3)$	2043/1992/1971/1926
$\text{Fe}_2[(\mu\text{-SCH}_2)_2\text{NCH}_2\text{CH}_2\text{CH}_2\text{SCH}_3](\text{CO})_5[\text{PPh}_2(2\text{-C}_5\text{H}_4\text{N})]$	2042/1992/1970/1933
$\text{Fe}_2[(\mu\text{-SCH}_2)_2\text{NCH}_2\text{CH}_2\text{CH}_2\text{SCH}_3](\text{CO})_5[\text{P}(\text{C}_6\text{H}_4\text{-4-CH}_3)_3]$	2042/1980/1928
$\text{Fe}_2[(\mu\text{-SCH}_2)_2\text{NC}_6\text{H}_4\text{-4-CH}_3](\text{CO})_5[\text{PPh}_2(2\text{-C}_5\text{H}_4\text{N})]$	2041/1993/1969/1924
$\text{Fe}_2[(\mu\text{-SCH}_2)_2\text{NC}_6\text{H}_4\text{-4-CH}_3](\text{CO})_5[\text{P}(\text{C}_6\text{H}_4\text{-4-CH}_3)_3]$	2044/1985/1930
$\text{Fe}_2[(\mu\text{-SCH}_2)_2\text{NCH}_2\text{CH}_2\text{PPh}_2](\text{CO})_5$	2041/1981/1951/1932
$\text{Fe}_2[(\mu\text{-SCH}_2)_2\text{O}](\text{CO})_5[\text{P}(\text{C}_6\text{H}_4\text{-4-F})_3]$	2052/1987/1940
$\text{Fe}_2[(\mu\text{-SCH}_2)_2\text{O}](\text{CO})_5[\text{P}(\text{C}_6\text{H}_4\text{-4-CH}_3)_3]$	2049/1988/1971/1935
$\text{Fe}_2[(\mu\text{-SCH}_2)_2\text{O}](\text{CO})_5[\text{PPh}_2(\text{CH}_2\text{CH}_3)]$	2046/1981/1929

frequency than those observed in the analogues $\text{Fe}_2[(\mu\text{-SCH}_2)_2\text{NR}](\text{CO})_6$.¹⁰ This indicates that the phosphine ligands (PPh_3 , $\text{PPh}_2(2\text{-C}_5\text{H}_4\text{N})$, $\text{P}(\text{C}_6\text{H}_4\text{-4-CH}_3)_3$, $\text{P}(\text{C}_6\text{H}_4\text{-4-F})_3$, $\text{PPh}_2(\text{CH}_2\text{CH}_3)$, and $-\text{CH}_2\text{CH}_2\text{PPh}_2$) are stronger electron donors than CO. Meanwhile, it can be seen from the first CO frequency of these different phosphine ligands in Table 2 that the electron-donating ability is described in the following: $\text{PPh}_2(2\text{-C}_5\text{H}_4\text{N}) > \text{P}(\text{C}_6\text{H}_4\text{-4-CH}_3)_3 > \text{PPh}_3$; $\text{PPh}_2(\text{CH}_2\text{CH}_3) > \text{P}(\text{C}_6\text{H}_4\text{-4-CH}_3)_3 > \text{P}(\text{C}_6\text{H}_4\text{-4-F})_3$.

The ^1H NMR spectra of 1–6 show two similar types of proton signals at ca. 2.80 and ca. 2.00 ppm assigned to the bridging dithiolate units ($\text{N}(\text{CH}_2\text{S})_2$), whereas those of 7 and 8

give two typical kinds of proton signals at ca. 4.00 and ca. 3.00 ppm for the $\text{N}(\text{CH}_2\text{S})_2$ groups. This is possibly due to the different substituent attached to the bridge head N atom, where complexes 1–6 contain the *alkyl*-substituted N atom, but complexes 7 and 8 have the *aryl*-linked N atom. In the ^1H spectrum of complex 9, the characteristic proton signals of the dithiolate bridging correspond to a multiplet in the range of 3.77–3.90 ppm. Furthermore, the ^{13}C NMR spectra of complexes 1–12 display a doublet at ca. 213 ppm for the coordinated Fe-carbonyls in $\text{PFe}(\text{CO})_2$ groups and a singlet at ca. 209 ppm for the terminal Fe-carbonyls in $\text{Fe}(\text{CO})_3$ moieties, respectively. Additionally, the ^{31}P NMR spectra of complexes 1–12 exhibit only a sharp singlet at 64.82, 66.75, 62.37, 64.85, 66.61, 62.44, 65.40, 62.07, 54.39, 61.83, 61.23, and 57.56 ppm attributed to the respective phosphorus atoms of the coordinated phosphine ligands, which are consistent with the X-ray analysis results.

Red single crystals of complexes 1–4, 6, 7, and 9–11 suitable for XRD analysis were obtained by slow vapor diffusion of hexane into the concentrated CH_2Cl_2 solution at 0 °C. As shown in Figures 2–4, the molecular structures of complexes

**Figure 2.** Molecular structure of complex 1. Hydrogens are omitted for clarity. Selected bond lengths [Å] and angles [°]: Fe1–Fe2 2.5304(7), P1–Fe2 2.2377(7), Fe2–Fe1–P1 151.963(17), C6–N1–C7 110.90(14).

1–3 all feature a butterfly $[2\text{Fe}_2\text{S}]$ cluster with five carbonyl ligands, an azadithiolate unit $[(\text{SCH}_2)_2\text{NCH}_2\text{CH}_2\text{CH}(\text{CH}_3)_2]$, and a phosphine ligand. In addition, two six-membered rings are formed in a chair-shaped and a boat-shaped configuration. It is interesting to note that the substituent of $-\text{CH}_2\text{CH}_2\text{CH}(\text{CH}_3)_2$ groups in complexes 1–3 are all attached to the bridge head N1 via the sterically favored equatorial bond, which are very similar to those reported in the diiron azadithiolate analogues $\text{Fe}_2[(\mu\text{-SCH}_2)_2\text{NCH}_2\text{CH}_2\text{OCH}_3](\text{CO})_6$,³⁷ $\text{Fe}_2[(\mu\text{-SCH}_2)_2\text{NCH}_2\text{CH}_2\text{O}_2\text{CCH}_2\text{CO}_2\text{CH}_2\text{CH}_3](\text{CO})_5(\text{PPh}_3)$,³⁸ and $\text{Fe}_2[(\mu\text{-SCH}_2)_2\text{NC}_6\text{H}_{11}](\text{CO})_4(\text{PMe}_3)_2$.³⁹ Moreover, the phosphorus atoms of the phosphine ligands (PPh_3 , $\text{PPh}_2(2\text{-C}_5\text{H}_4\text{N})$, $\text{P}(\text{C}_6\text{H}_4\text{-4-CH}_3)_3$) are all bound in apical positions. The Fe1–Fe2 bond lengths in 1 (2.5304(7) Å, Figure 2), 2 (2.5330(5) Å, Figure 3), and 3 (2.5159(6) Å, Figure 4) are slightly shorter than the corresponding lengths (2.55–2.62 Å) in the natural enzymes.⁷ Meanwhile, the order of the Fe–P bond lengths for complexes 1–3 is shown as follows: 1 (P1–Fe2, 2.2377(7) Å) > 3 (P1–Fe2, 2.2366(6) Å) > 2 (P1–Fe2, 2.2328(5) Å), indicating the electron-donating ability of $\text{PPh}_2(2\text{-C}_5\text{H}_4\text{N}) > \text{P}(\text{C}_6\text{H}_4\text{-4-CH}_3)_3 > \text{PPh}_3$, which is consistent with the results observed in the IR spectra of complexes 1–3. The Fe–Fe–P bond angles in 3 (Fe2–Fe1–P1 155.228°) are bigger than the corresponding angles in 1 (Fe2–Fe1–P1 151.963°) and 2

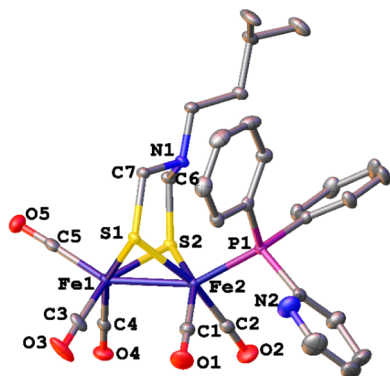


Figure 3. Molecular structure of complex 2. Hydrogens are omitted for clarity. Selected bond lengths [Å] and angles [°]: Fe1–Fe2 2.5330(5), P1–Fe2 2.2328(5), Fe1–Fe2–P1 151.131(17), C6–N1–C7 110.46(13).

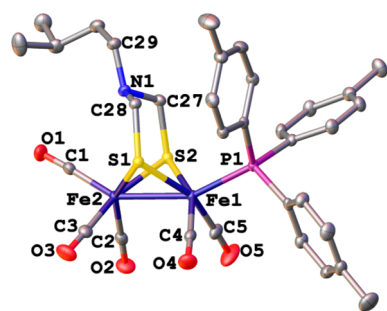


Figure 4. Molecular structure of complex 3. Hydrogens are omitted for clarity. Selected bond lengths [Å] and angles [°]: Fe1–Fe2 2.5159(6), P1–Fe2 2.2366(6), Fe2–Fe1–P1 155.228(18), C27–N1–C28 110.88(15).

(Fe2–Fe1–P1 151.131°), which demonstrated that the steric hindrance between the bridge-N substituent (NCH₂CH₂CH(CH₃)₂) and the phosphine ligand (P(C₆H₄-4-CH₃)₃) in 3 is bigger relative to those in 1 and 2 as observed in Figures 2–4.

As shown in Figures 5 and 6, the Fe1–Fe2 distances in 4 and 6 are 2.5277(4) Å (Figure 5) and 2.5305(4) Å (Figure 6) respectively, which are also shorter than that observed in the active site of [FeFe] hydrogenase. As shown in Figures 5 and 6, the stereochemistry of the two Fe(CO)₂P sites exhibits that two CO groups occupy the basal site and the Lewis basic phosphine

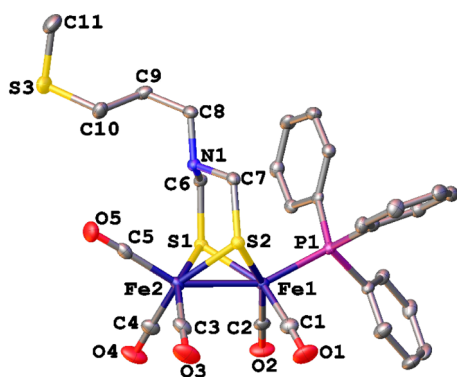


Figure 5. Molecular structure of complex 4. Hydrogens are omitted for clarity. Selected bond lengths [Å] and angles [°]: Fe1–Fe2 2.5277(4), P1–Fe1 2.2398(5), P1–Fe1–Fe2 153.632(17), C6–N1–C7 111.70(14), C6–N1–C8 109.33(14), C7–N1–C8 108.63(14).

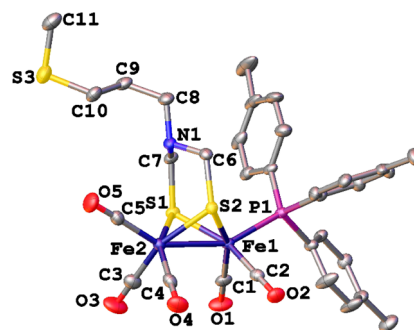


Figure 6. Molecular structure of complex 6. Hydrogens are omitted for clarity. Selected bond lengths [Å] and angles [°]: Fe1–Fe2 2.5305(4), Fe1–P1 2.2371(6), P1–Fe1–Fe2 153.843(19), C6–N1–C7 111.75(16), C6–N1–C8 108.69(16), C7–N1–C8 109.21(16).

ligand lies in the apical site. It is worth noting that the substituent of the –CH₂CH₂CH₂SMe group in complexes 4 and 6 is attached to the bridge head N1 via the sterically favored equatorial bond.

As shown in Figure 7, complex 7 exhibits a typical butterfly [2Fe₂S] core, whereas the geometry around each iron atoms

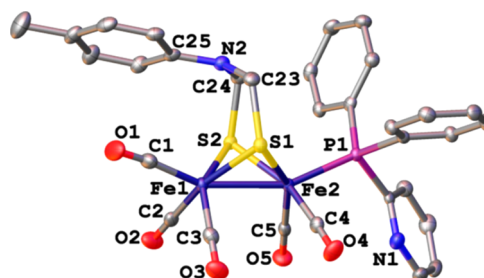


Figure 7. Molecular structure of complex 7. Hydrogens and solvents are omitted for clarity. Selected bond lengths [Å] and angles [°]: Fe1–Fe2 2.5104(4), Fe2–P1 2.2373(6), P1–Fe2–Fe1 156.870(19), C23–N2–C24 113.24(17), C23–N2–C25 121.93(17), C24–N2–C25 118.83(17).

can be described as a distorted square pyramidal. It is worth noting that the sum of angles around N1 atom is 354°, demonstrating that the amine is planar. This is good agreement with the fact that p-π conjugation with the p-orbital of the nitrogen is reflected by short N–C distance, which is very similar to those reported in the corresponding analogues Fe₂[(μ-SCH₂)₂NC₆H₄-4-CF₃](CO)₅(PPh₃),²⁸ Fe₂[(μ-SCH₂)₂NC₆F₄-4-CF₃](CO)₅(PPh₃),²⁸ and Fe₂[(μ-SCH₂)₂NC₆H₄SO₃Na](CO)₅(PPh₃).⁴⁰

As shown in Figure 8, the crystal structure of complex 9 reveals that phosphorus atom is coordinated to one Fe(1) core, which is consistent with the corresponding carbonyl frequencies observed in the IR data of complex 9. The Fe1–Fe2 bond and Fe1–P1 bond lengths in 9 (2.5113(3) and 2.2155(5) Å) are very close to those of complexes 1–4 and 6. However, in contrast to complexes 1–4 and 6, the substituent of the –CH₂CH₂PPh₂ group attached to the bridge head N1 resides in an axial position due to the formation of the seven-membered ring (FeSCNCCP). It is worth pointing out that complex 9 is structurally similar to the known [2Fe₃S] complex Fe₂[(μ-SCH₂)₂NCH₂CH₂SCH₃](CO)₅.³³

As shown in Figures 9 and 10, both complexes 10 and 11 feature a butterfly [2Fe₂S] cluster with five carbonyl ligands, an oxadithiolate unit (CH₂OCH₂), and a phosphine ligand

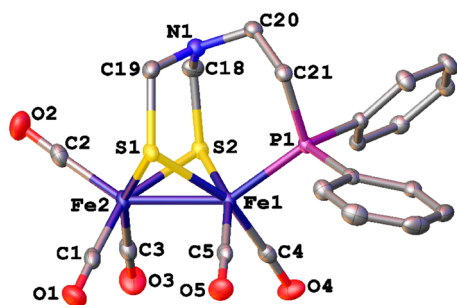


Figure 8. Molecular structure of complex **9**. Hydrogens and solvents are omitted for clarity. Selected bond lengths [Å] and angles [°]: Fe1–Fe2 2.5113(3), Fe1–P1 2.2155(5), P1–Fe1–Fe2 1145.898(16), C18–N1–C19 115.63(14), C18–N1–C20 120.65(14), C19–N1–C20 118.30(14).

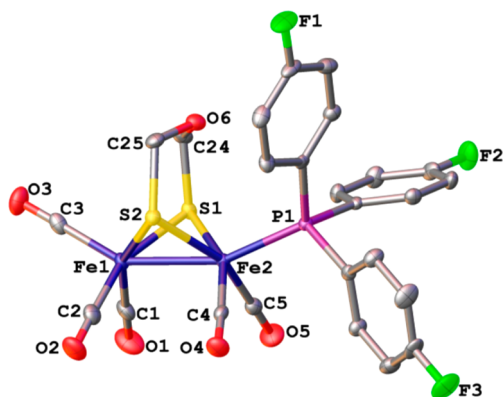


Figure 9. Molecular structure of complex **10**. Hydrogens and solvents are omitted for clarity. Selected bond lengths [Å] and angles [°]: Fe1–Fe2 2.5174(7), Fe2–P1 2.2470(10), P1–Fe2–Fe1 157.08(3), C24–O6–C25 112.6(2).

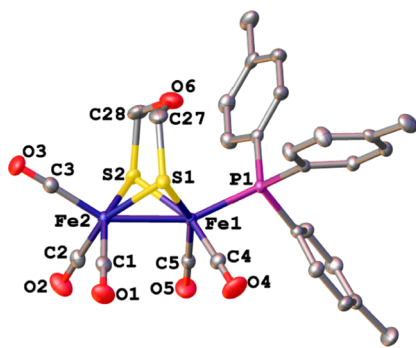


Figure 10. Molecular structure of complex **11**. Hydrogens and solvents are omitted for clarity. Selected bond lengths [Å] and angles [°]: Fe1–Fe2 2.5261(5), Fe1–P1 2.2462(7), P1–Fe1–Fe2 155.464(19), C27–O6–C28 113.9(2).

($P(C_6H_4-4-F)_3$, $P(C_6H_4-4-CH_3)_3$). Two six-membered rings are formed in a chair-shaped and a boat-shaped configuration. The phosphorus atoms of the phosphine ligands are both bound in apical positions, which are very similar to the reported diiron oxadithiolate complexes such as $Fe_2[(\mu-SCH_2)_2O](CO)_5(Ph_2PCl)$ and $Fe_2[(\mu-SCH_2)_2O](CO)_5(Ph_2PNMe_2)$.⁴¹ In addition, the Fe–P bond lengths for complexes **10** and **11** are 2.2470(10) Å and 2.2462(7) Å, indicating that the electron-donating ability of $P(C_6H_4-4-F)_3 < P(C_6H_4-4-CH_3)_3$. The Fe–Fe–P bond angles in **10** (Fe2–Fe1–P1 157.08(3)°)

are bigger than the corresponding angles in **1** (Fe2–Fe1–P1 151.963°) and **11** (Fe2–Fe1–P1 155.464(19)°).

Electrochemical Studies of Complexes 1–6 and 10. The electrochemical properties of complexes **1–6** were studied by CV in DCM solution. The electrochemical data of complexes **1–6** and **10** are listed in Table 3. The CV curve

Table 3. Electrochemical Data of Complexes **1–6** and **10**

complex	E_{pc1} [V]	E_{pa} [V]
1	−2.04	+0.26
2	−2.08	+0.18
3	−2.10	+0.22
4	−2.05	+0.25
5	−2.06	+0.17
6	−2.10	+0.23
10	−1.94	+0.54

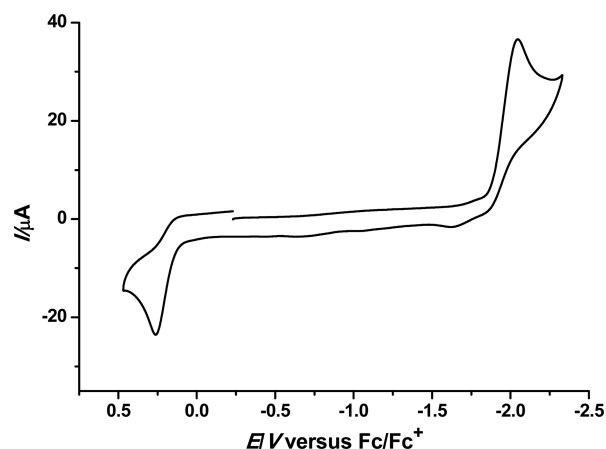


Figure 11. Cyclic voltammogram of complex **1** (1.0 mM) in 0.1 M $n\text{-Bu}_4\text{NPF}_6/\text{DCM}$ at a scan rate of 100 mV s^{-1} .

of complex **1** is shown in Figure 11, whereas the CV curves of complexes **1** and **10** are displayed in Figures 12 and 13. As shown in Figure 11, complex **1** displays one irreversible reduction process at -2.04 V and one irreversible oxidation process at $+0.26 \text{ V}$, which can be ascribed to the reduction of

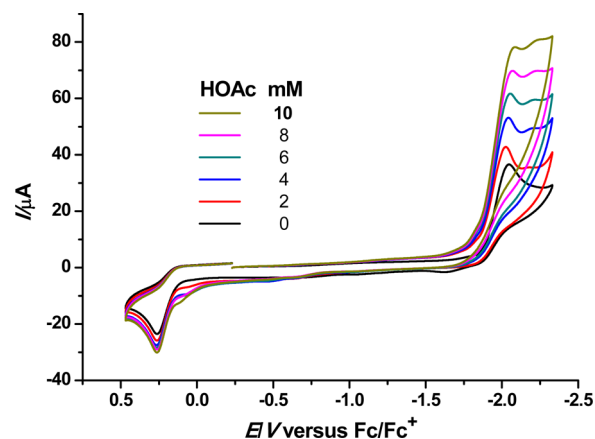


Figure 12. Cyclic voltammogram of complex **1** (1.0 mM) with HOAc (0–10 mM) in 0.1 M $n\text{-Bu}_4\text{NPF}_6/\text{DCM}$ at a scan rate of 100 mV s^{-1} .

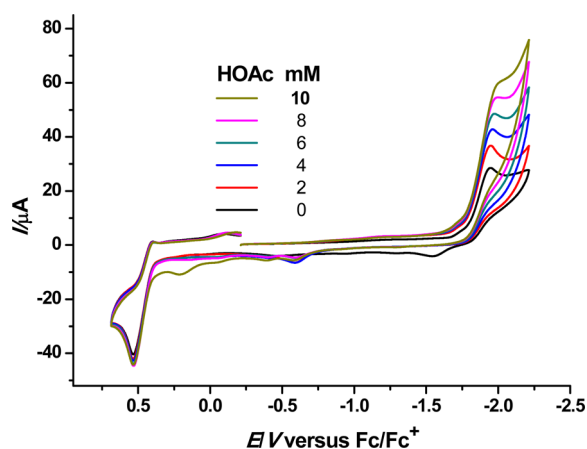


Figure 13. Cyclic voltammogram of complex **10** (1.0 mM) with HOAc (0–10 mM) in 0.1 M *n*-Bu₄NPF₆/DCM at a scan rate of 100 mV s⁻¹.

Fe^IFe^I to Fe^IFe⁰ and the oxidation of Fe^IFe^I to Fe^{II}Fe^{II},^{42–44} respectively. In addition, complexes **1** and **10** have been found to have the catalytic ability for proton reduction to H₂ in the presence of HOAc under CV conditions. As shown in Figures 12 and 13, upon addition of the first 2 mM HOAc to the solutions of complexes **1** and **10**, the reduction peaks at -2.04 V and -1.94 V increased markedly and continued to increase with increasing concentration of HOAc. These observations imply that complexes **1** and **10** have the ability to the electrocatalytic reduction of proton to dihydrogen. In addition, according to the above-mentioned electrochemical observations of complexes **1** and **10**, a 2E2C (E = electrochemical; C = chemical) catalytic mechanism can be proposed for this electrocatalytic H₂ production. We suggest that complexes **1** and **10** may be completed via the EC/EC or EC/CE catalytic mechanism, although more evidence is still needed for an accurate mechanism.

EXPERIMENTAL DETAILS

Reactions were performed using standard Schlenk techniques. Solvents were distilled under nitrogen over an appropriate drying agent. LiHBEt₃ (1.0 M in THF), HCHO (37%), NH₂CH₂CH₂CH(CH₃)₂, NH₂CH₂CH₂CH₂SCH₃, NH₂C₆H₄-4-CH₃, Ph₂PCH₂CH₂NH₂, PPh₃, PPh₂(2-C₅H₄N), P(C₆H₄-4-CH₃)₃, P(C₆H₄-4-F)₃, and PPh₂(CH₂CH₃) were obtained commercially and used as received. Complex Fe₂(μ-S)₂(CO)₆ was prepared according to the literature procedures.⁴⁵ Preparative TLC was carried out on glass plates (26 × 20 × 0.25 cm) coated with silica gel H (10–40 μm). ¹H NMR spectra (500 MHz) were referenced to residual solvent relative to tetramethylsilane. ³¹P NMR (202 MHz) spectra were referenced to external 85% H₃PO₄. IR spectra were recorded at room temperature on a Bruker Vector 22 infrared spectrophotometer. Elemental analyses were performed on an Elementar Vario EL analyzer. Crystallographic data for complexes **1–4**, **6**, **7**, and **9–11** were collected using a Bruker SMART diffractometer equipped with a Mo Kα source (λ = 0.71073 Å). Data collection, reduction, and absorption corrections were performed by Bruker SMART and Bruker SAINT. The structures were solved by direct methods using the SHELXS-97 program and refined by full-matrix least-squares techniques (SHELXL-97) on F².^{46,47} Hydrogen atoms were located using the geometric method. Electrochemical measurements were carried out under nitrogen using a CHI 620 Electrochemical Workstation. As the electrolyte, *n*-Bu₄NPF₆ was recrystallized multiple times from a CH₂Cl₂ solution by the addition of hexane. CV scans were obtained in a three-electrode cell with a glassy carbon electrode (3 mm diameter) as the working electrode, a platinum wire as the counter electrode, and a nonaqueous Ag/Ag⁺

electrode as the reference electrode. The potential scale was calibrated against the Fc/Fc⁺ couple and reported versus this reference system.

Synthesis of Complex Fe₂[(μ-SCH₂)₂NCH₂CH₂CH(CH₃)₂](CO)₆(PPh₃) (1**).** *Method A.* The reaction was carried out under nitrogen atmosphere by use of standard Schlenk techniques. A red solution of Fe₂(μ-S)₂(CO)₆ (0.344 g, 1.0 mmol) in THF (15 mL) was cooled to -78 °C and then treated dropwise with LiHBEt₃ (2 mL, 2.0 mmol) to give a green solution. After stirring for 10 min, CF₃CO₂H (0.16 mL, 2.0 mmol) was added to cause an immediate color change from green to red. The mixture was stirred for 10 min, and then 37% aqueous formaldehyde (0.17 mL, 2.0 mmol) was added. The new mixture was allowed to warm up to room temperature and stirred for 2 h. Then PPh₃ (0.262 g, 1.0 mmol) was added to cause an immediate color change from red to dark red. After stirring for 4 h, NH₂CH₂CH₂CH(CH₃)₂ (0.12 mL, 1.0 mmol) was added, and the resulting solution was stirred for additional 12 h. Volatiles were removed under vacuum, and the residue was subjected to TLC using CH₂Cl₂/petroleum ether (v/v = 1:4) as eluent. From the main red band, complex **1** (0.221 g, 56%) was obtained as a dark red solid. Anal. calcd for C₃₀H₃₀Fe₂NO₃PS₂: C, 52.12; H, 4.37; N, 2.03. Found: C, 51.87; H, 4.51; N, 1.98. IR (KBr disk): ν_{C=O} 2040 (vs), 1984 (vs), 1976 (vs), 1932 (m) cm⁻¹. ¹H NMR (δ, ppm, 500 MHz, CDCl₃): 7.68 (s, 6H, 3*m*-PhH), 7.42 (s, 9H, 3*o*, *p*-PhH), 2.79 (s, 2H, 2NCH₂H_sS), 2.38 (s, 2H, NCH₂CH₂), 1.98 (s, 2H, NCH₃H_sS), 1.25 (s, 1H, CH), 0.83 (s, 2H, NCH₂CH₂), 0.71 (s, 6H, 2CH₃). ¹³C NMR (δ, ppm, 126 MHz, TMS): 22.43 (CH₃), 26.09 (NCH₂CH₂), 34.72 (CH), 50.80 (NCH₂CH₂), 57.01 (NCH₂S), 128.35, 129.97, 133.51, 136.00 (PhCH), 209.78 (s, FeCO), 213.61 (d, ²J_{PC} = 8.9 Hz, PFeCO). ³¹P NMR (202 MHz, CDCl₃, 85% H₃PO₄): 64.82 (s).

Method B. (i) A red solution of Fe₂(μ-S)₂(CO)₆ (0.344 g, 1.0 mmol) in THF (15 mL) was cooled to -78 °C and then treated dropwise with LiHBEt₃ (2 mL, 2.0 mmol) to give a green solution. After stirring for 10 min, CF₃CO₂H (0.16 mL, 2.0 mmol) was added to cause an immediate color change from green to red. The mixture was stirred for 10 min, and then 37% aqueous formaldehyde (0.17 mL, 2.0 mmol) was added. The new mixture was allowed to warm up to room temperature and stirred for 2 h. Then NH₂CH₂CH₂CH(CH₃)₂ (0.12 mL, 1.0 mmol) was added, and the resulting solution was stirred for additional 6 h. Volatiles were removed under vacuum, and the residue was subjected to TLC using CH₂Cl₂/petroleum ether (v/v = 1:4) as eluent. From the main red band, complex Fe₂[(μ-SCH₂)₂NCH₂CH₂CH(CH₃)₂](CO)₆ (0.200 g) was obtained as a red solid. IR (KBr disk): ν_{C=O} 2073 (vs), 2030 (vs), 1995 (vs) cm⁻¹. ¹H NMR (δ, ppm, 500 MHz, CDCl₃): 3.47 (s, 4H, 2NCH₂S), 2.63 (s, 2H, NCH₂CH₂), 1.46 (s, 1H, CH), 1.18 (s, 2H, NCH₂CH₂), 0.85 (s, 6H, 2CH₃). ¹³C NMR (δ, ppm, 126 MHz, TMS): 22.43 (CH₃), 25.75 (NCH₂CH₂), 36.29 (CH), 52.98 (NCH₂CH₂), 55.67 (NCH₂S), 207.81 (s, FeCO). (ii) To a solution of complex Fe₂[(μ-SCH₂)₂NCH₂CH₂CH(CH₃)₂](CO)₆ (0.200 g, 0.44 mmol) in CH₃CN (15 mL) was added decarbonylation reagent Me₃NO·2H₂O (0.049 g, 0.44 mmol). The mixture was stirred at room temperature for 15 min, and then PPh₃ (0.116 g, 0.44 mmol) was added. The resulting mixture was stirred for additional 2 h to give a dark red solution. Solvents were removed under vacuum, and the residue was subjected to TLC using CH₂Cl₂/petroleum ether (v/v = 1:4) as eluent. From the main red band, complex **1** (0.160 g, 23%, calculated by Fe₂(μ-S)₂(CO)₆) was obtained as a dark red solid.

Synthesis of Complex Fe₂[(μ-SCH₂)₂NCH₂CH₂CH(CH₃)₂](CO)₆[PPh₂(2-C₅H₄N)] (2**).** Complex **2** was prepared in a fashion similar to that of complex **1** (Methods A and B) using PPh₂(2-C₅H₄N) as the phosphine ligand. Yields: 43% (Method A) and 21% (Method B), dark red solid. Anal. calcd for C₂₉H₂₉Fe₂N₃O₃PS₂: C, 50.31; H, 4.22; N, 4.05. Found: C, 50.25; H, 4.39; N, 3.86. IR (KBr disk): ν_{C=O} 2038 (vs), 1987 (vs), 1970 (vs), 1955 (vs) cm⁻¹. ¹H NMR (δ, ppm, 500 MHz, CDCl₃): 7.44–8.81 (m, 14H, 2PhH, C₅H₄N), 2.79 (s, 2H, 2NCH₂H_sS), 2.54 (s, 2H, NCH₂CH₂), 2.03 (s, 2H, 2NCH₃H_sS), 1.26 (s, 1H, CH), 0.82 (s, 2H, NCH₂CH₂), 0.72 (s, 6H, 2CH₃). ¹³C NMR (δ, ppm, 126 MHz, TMS): 21.44 (CH₃), 25.10 (NCH₂CH₂), 33.87 (CH), 50.08 (NCH₂CH₂), 55.92 (NCH₂S), 122.29, 126.38, 127.25, 129.13, 133.08, 133.91, 134.41, 148.97, 160.87 (PhCH, C₅H₄N),

208.89 (s, FeCO), 212.33 (d, $^2J_{\text{PC}} = 10.2$ Hz, PFeCO). ^{31}P NMR (202 MHz, CDCl_3 , 85% H_3PO_4): 66.75 (s).

Synthesis of Complex $\text{Fe}_2[(\mu\text{-SCH}_2)_2\text{NCH}_2\text{CH}_2\text{CH}(\text{CH}_3)_2]\text{-(CO)}_5[\text{P}(\text{C}_6\text{H}_4\text{-4-CH}_3)_3]$ (3). Complex 3 was prepared in a fashion similar to that of complex 1 (Methods A and B) using $\text{P}(\text{C}_6\text{H}_4\text{-4-CH}_3)_3$ as the phosphine ligand. Yields: 51% (Method A) and 24% (Method B), dark red solid. Anal. calcd for $\text{C}_{33}\text{H}_{36}\text{Fe}_2\text{NO}_5\text{PS}_2$: C, 54.04; H, 4.95; N, 1.91. Found: C, 53.95; H, 5.12; N, 1.95. IR (KBr disk): $\nu_{\text{C}=\text{O}}$ 2038 (vs), 1988 (vs), 1969 (vs), 1955 (vs) cm^{-1} . ^1H NMR (δ , ppm, 500 MHz, CDCl_3): 7.55 (s, 6H, 3*m*-PhH), 7.21 (s, 6H, 3*o*-PhH), 2.80 (d, $J = 10$ Hz, 2H, $2\text{NCH}_2\text{H}_e\text{S}$), 2.37 (s, 11H, 3CH₃, NCH_2CH_2), 2.04 (s, 2H, $2\text{NCH}_2\text{H}_e\text{S}$), 1.26 (s, 1H, CH), 0.82 (s, 2H, NCH_2CH_2), 0.71 (d, $J = 5$ Hz, 6H, 2CH₃). ^{13}C NMR (δ , ppm, 126 MHz, TMS): 21.30 (CH₂CH₃), 22.43 (CH₃), 26.06 (NCH₂CH₂), 34.83 (CH), 50.77 (NCH₂CH₂), 56.99 (NCH₂S), 129.03, 133.47, 140.04 (PhCH), 210.02 (s, FeCO), 213.88 (d, $^2J_{\text{PC}} = 10.9$ Hz, PFeCO). ^{31}P NMR (202 MHz, CDCl_3 , 85% H_3PO_4): 62.37 (s).

Synthesis of Complex $\text{Fe}_2[(\mu\text{-SCH}_2)_2\text{NCH}_2\text{CH}_2\text{CH}_2\text{SCH}_3]\text{-(CO)}_5[\text{PPh}_3]$ (4). Complex 4 was prepared in a fashion similar to that of complex 1 (Methods A and B) using $\text{NH}_2\text{CH}_2\text{CH}_2\text{CH}_2\text{SCH}_3$ as the amine. Yields: 42% (Method A) and 20% (Method B), dark red solid. Anal. calcd for $\text{C}_{29}\text{H}_{28}\text{Fe}_2\text{NO}_5\text{PS}_3$: C, 49.10; H, 3.98; N, 1.97. Found: C, 48.81; H, 4.22; N, 1.91. IR (KBr disk): $\nu_{\text{C}=\text{O}}$ 2043 (vs), 1992 (vs), 1971 (vs), 1926 (s) cm^{-1} . ^1H NMR (δ , ppm, 500 MHz, CDCl_3): 7.43–7.68 (m, 15H, 3PhH), 2.88 (d, $J = 11$ Hz, 2H, $2\text{NCH}_2\text{H}_e\text{S}$), 2.34 (brs, 2H, $\text{NCH}_2\text{CH}_2\text{CH}_2\text{S}$), 2.22 (s, 2H, $\text{NCH}_2\text{CH}_2\text{CH}_2\text{S}$), 2.15 (br s, 2H, $2\text{NCH}_2\text{H}_e\text{S}$), 1.98 (s, 3H, SCH₃), 1.30 (br s, 2H, $\text{NCH}_2\text{CH}_2\text{CH}_2\text{S}$). ^{13}C NMR (δ , ppm, 126 MHz, TMS): 15.41 (SCH₃), 25.52 (NCH₂CH₂CH₂S), 31.56 (NCH₂CH₂CH₂S), 50.56 (NCH₂CH₂CH₂S), 57.18 (NCH₂S), 128.40, 130.05, 133.50, 135.79 (C₆H₅), 209.77 (s, FeCO), 213.49 (d, $^2J_{\text{PC}} = 10.2$ Hz, PFeCO). ^{31}P NMR (202 MHz, CDCl_3 , 85% H_3PO_4): 64.85 (s).

Synthesis of Complex $\text{Fe}_2[(\mu\text{-SCH}_2)_2\text{NCH}_2\text{CH}_2\text{CH}_2\text{SCH}_3]\text{-(CO)}_5[\text{PPh}_2(2\text{-C}_5\text{H}_4\text{N})]$ (5). Complex 5 was prepared in a fashion similar to that of complex 2 using $\text{NH}_2\text{CH}_2\text{CH}_2\text{CH}_2\text{SCH}_3$ as the amine. Yields: 45% (Method A) and 20% (Method B), dark red solid. Anal. calcd for $\text{C}_{28}\text{H}_{27}\text{Fe}_2\text{N}_2\text{O}_5\text{PS}_3$: C, 47.34; H, 3.83; N, 3.94. Found: C, 47.25; H, 3.86; N, 4.01. IR (KBr disk): $\nu_{\text{C}=\text{O}}$ 2042 (vs), 1992 (vs), 1970 (vs), 1933 (m) cm^{-1} . ^1H NMR (δ , ppm, 500 MHz, CDCl_3): 7.44–8.81 (m, 14H, 2PhH, C₅H₄N), 2.89 (d, $J = 10.5$ Hz, 2H, $2\text{NCH}_2\text{H}_e\text{S}$), 2.52 (d, 2H, $J = 8.5$ Hz, $\text{NCH}_2\text{CH}_2\text{CH}_2\text{S}$), 2.21–2.24 (m, 4H, $\text{NCH}_2\text{CH}_2\text{CH}_2\text{S}$, $2\text{NCH}_2\text{H}_e\text{S}$), 1.99 (s, 3H, SCH₃), 1.30 (s, 2H, $\text{NCH}_2\text{CH}_2\text{CH}_2\text{S}$). ^{13}C NMR (δ , ppm, 126 MHz, TMS): 15.42 (SCH₃), 25.61 (NCH₂CH₂CH₂S), 31.59 (NCH₂CH₂CH₂S), 50.85 (NCH₂CH₂CH₂S), 57.09 (NCH₂S), 123.35, 127.35, 128.31, 132.39, 134.07, 134.78, 135.66, 149.95, 161.68 (C₆H₅, C₅H₄N), 209.88 (s, FeCO), 213.20 (d, $^2J_{\text{PC}} = 10.5$ Hz, PFeCO). ^{31}P NMR (202 MHz, CDCl_3 , 85% H_3PO_4): 66.61 (s).

Synthesis of Complex $\text{Fe}_2[(\mu\text{-SCH}_2)_2\text{NCH}_2\text{CH}_2\text{CH}_2\text{SCH}_3]\text{-(CO)}_5[\text{P}(\text{C}_6\text{H}_4\text{-4-CH}_3)_3]$ (6). Complex 6 was prepared in a fashion similar to that of complex 3 using $\text{NH}_2\text{CH}_2\text{CH}_2\text{CH}_2\text{SCH}_3$ as the amine. Yields: 41% (Method A) and 19% (Method B), dark red solid. Anal. calcd for $\text{C}_{32}\text{H}_{34}\text{Fe}_2\text{NO}_5\text{PS}_3$: C, 51.15; H, 4.56; N, 1.86. Found: C, 50.88; H, 4.75; N, 1.83. IR (KBr disk): $\nu_{\text{C}=\text{O}}$ 2042 (vs), 1980 (vs), 1928 (m) cm^{-1} . ^1H NMR (δ , ppm, 500 MHz, CDCl_3): 7.54 (t, $J = 9.5$ Hz, 6H, 3*m*-PhH), 7.20 (d, $J = 7.5$ Hz, 6H, 3*o*-PhH), 2.90 (d, $J = 11.5$ Hz, 2H, $2\text{NCH}_2\text{H}_e\text{S}$), 2.38 (br s, 11H, 3CH₃, $\text{NCH}_2\text{CH}_2\text{CH}_2\text{S}$), 2.21–2.24 (m, 4H, $\text{NCH}_2\text{CH}_2\text{CH}_2\text{S}$, $2\text{NCH}_2\text{H}_e\text{S}$), 1.98 (s, 3H, SCH₃), 1.30 (s, 2H, $\text{NCH}_2\text{CH}_2\text{CH}_2\text{S}$). ^{13}C NMR (δ , ppm, 126 MHz, TMS): 15.41 (SCH₃), 21.31 (CH₃), 25.76 (NCH₂CH₂CH₂S), 31.66 (NCH₂CH₂CH₂S), 50.68 (NCH₂CH₂CH₂S), 57.17 (NCH₂S), 129.08, 133.50, 140.16 (PhCH), 210.00 (s, FeCO), 213.80 (d, $^2J_{\text{PC}} = 11.3$ Hz, PFeCO). ^{31}P NMR (202 MHz, CDCl_3 , 85% H_3PO_4): 62.44 (s).

Synthesis of Complex $\text{Fe}_2[(\mu\text{-SCH}_2)_2\text{NC}_6\text{H}_4\text{-4-CH}_3]\text{-(CO)}_5[\text{PPh}_2(2\text{-C}_5\text{H}_4\text{N})]$ (7). Complex 7 was prepared in a fashion similar to that of complex 2 using $\text{NH}_2\text{C}_6\text{H}_4\text{-4-CH}_3$ as the amine. Yields: 31% (Method A) and 16% (Method B), dark red solid. Anal. calcd for $\text{C}_{31}\text{H}_{25}\text{Fe}_2\text{N}_2\text{O}_5\text{PS}_2$: C, 52.27; H, 3.54; N, 3.93. Found: C,

51.99; H, 3.75; N, 3.91. IR (KBr disk): $\nu_{\text{C}=\text{O}}$ 2041 (vs), 1993 (vs), 1969 (vs), 1924 (m) cm^{-1} . ^1H NMR (δ , ppm, 500 MHz, CDCl_3): 6.47–8.82 (m, 18H, 2PhH, C₆H₄, C₅H₄N), 3.99 (d, $J = 7.0$ Hz, 2H, $2\text{NCH}_2\text{H}_e\text{S}$), 3.29 (br s, 2H, $2\text{NCH}_2\text{H}_e\text{S}$), 2.24 (s, 3H, CH₃). ^{13}C NMR (δ , ppm, 126 MHz, TMS): 20.33 (CH₃), 47.92 (NCH₂S), 115.87, 118.17, 123.50, 128.53, 128.31, 130.16, 134.14, 144.54, 150.01 (C₆H₅, C₅H₄N), 208.99 (s, FeCO), 212.78 (d, $^2J_{\text{PC}} = 10.6$ Hz, PFeCO). ^{31}P NMR (202 MHz, CDCl_3 , 85% H_3PO_4): 65.4 (s).

Synthesis of Complex $\text{Fe}_2[(\mu\text{-SCH}_2)_2\text{NC}_6\text{H}_4\text{-4-CH}_3]\text{-(CO)}_5[\text{P}(\text{C}_6\text{H}_4\text{-4-CH}_3)_3]$ (8). Complex 8 was prepared in a fashion similar to that of complex 3 using $\text{NH}_2\text{C}_6\text{H}_4\text{-4-CH}_3$ as the amine. Yields: 33% (Method A) and 17% (Method B), dark red solid. Anal. calcd for $\text{C}_{35}\text{H}_{32}\text{Fe}_2\text{NO}_5\text{PS}_2$: C, 55.80; H, 4.28; N, 1.86. Found: C, 55.70; H, 4.44; N, 1.81. IR (KBr disk): $\nu_{\text{C}=\text{O}}$ 2044 (vs), 1985 (vs), 1930 (m) cm^{-1} . ^1H NMR (δ , ppm, 500 MHz, CDCl_3): 7.63 (t, $J = 8.5$ Hz, 6H, 3*m*-PhH), 7.20 (d, $J = 6.5$ Hz, 6H, 3*o*-PhH), 7.03 (d, $J = 7.0$ Hz, 2H, $2\text{-NC}_6\text{H}_4\text{-4-CH}_3$), 6.51 (d, $J = 7.5$ Hz, 2H, $2\text{m-NC}_6\text{H}_4\text{-4-CH}_3$), 4.00 (d, $J = 12.5$ Hz, 2H, $2\text{NCH}_2\text{H}_e\text{S}$), 3.04 (br s, 2H, $2\text{NCH}_2\text{H}_e\text{S}$), 2.42 (s, 9H, 3C₆H₄-4-CH₃), 2.26 (s, 3H, NC₆H₄-4-CH₃). ^{13}C NMR (δ , ppm, 126 MHz, TMS): 20.33 (NC₆H₄-4-CH₃), 21.31 (C₆H₄-4-CH₃), 47.45 (NCH₂S), 115.81, 129.26, 129.91, 132.39, 132.72, 133.52, 140.38, 144.49 (PhCH), 209.07 (s, FeCO), 213.24 (d, $^2J_{\text{PC}} = 11.3$ Hz, PFeCO). ^{31}P NMR (202 MHz, CDCl_3 , 85% H_3PO_4): 62.07 (s).

Synthesis of Complex $\text{Fe}_2[(\mu\text{-SCH}_2)_2\text{NCH}_2\text{CH}_2\text{PPh}_2]\text{-(CO)}_5$ (9). A red solution of $\text{Fe}_2(\mu\text{-S})_2(\text{CO})_6$ (0.344 g, 1.0 mmol) in THF (15 mL) was cooled to -78 °C and then treated dropwise with LiHBET₃ (2 mL, 2.0 mmol) to give a green solution. After stirring for 10 min, $\text{CF}_3\text{CO}_2\text{H}$ (0.16 mL, 2.0 mmol) was added to cause an immediate color change from green to red. The mixture was stirred for 10 min, and then 37% aqueous formaldehyde (0.17 mL, 2.0 mmol) was added. The new mixture was allowed to warm up to room temperature and stirred for 2 h. Then $\text{Ph}_2\text{PCH}_2\text{CH}_2\text{NH}_2$ (0.23 g, 1.0 mmol) was added, and the resulting solution was stirred for 12 h. Volatiles were removed under vacuum, and the residue was subjected to TLC using CH_2Cl_2 /petroleum ether ($v/v = 1:2$) as eluent. From the main red band, complex 9 (0.135 g, 24%) was obtained as a dark red solid. Anal. calcd for $\text{C}_{21}\text{H}_{18}\text{Fe}_2\text{NO}_5\text{PS}_2$: C, 44.16; H, 3.18; N, 2.45. Found: C, 44.12; H, 3.27; N, 2.38. IR (KBr disk): $\nu_{\text{C}=\text{O}}$ 2041 (vs), 1981 (vs), 1951 (s), 1932 (m) cm^{-1} . ^1H NMR (δ , ppm, 500 MHz, CDCl_3): 7.50–7.81 (m, 10H, PhH), 3.77–3.90 (m, 4H, $2\text{NCH}_2\text{S}$), 2.79–2.89 (m, 4H, $\text{NCH}_2\text{CH}_2\text{P}$). ^{13}C NMR (δ , ppm, 126 MHz, TMS): 37.38 (NCH₂CH₂), 50.79 (NCH₂CH₂), 53.38 (NCH₂S), 128.35, 129.97, 133.51, 136.00 (PhCH), 209.40 (s, FeCO), 212.10 (d, $^2J_{\text{PC}} = 6.9$ Hz, PFeCO). ^{31}P NMR (202 MHz, CDCl_3 , 85% H_3PO_4): 54.39 (s).

Synthesis of Complex $\text{Fe}_2[(\mu\text{-SCH}_2)_2\text{O}]\text{-(CO)}_5[\text{P}(\text{C}_6\text{H}_4\text{-4-F})_3]$ (10). A red solution of $\text{Fe}_2(\mu\text{-S})_2(\text{CO})_6$ (0.344 g, 1.0 mmol) in THF (20 mL) was cooled to -78 °C and then treated dropwise with LiHBET₃ (2 mL, 2.0 mmol) to give a green solution. After stirring for 15 min, $\text{CF}_3\text{CO}_2\text{H}$ (0.18 mL, 2.2 mmol) was added to cause an immediate color change from green to red. The mixture was stirred for 10 min, and then 37% aqueous formaldehyde (0.17 mL, 2.0 mmol) was added. The new mixture was allowed to warm up to room temperature and stirred at this temperature for 1 h. Then $\text{P}(\text{C}_6\text{H}_4\text{-4-F})_3$ (0.316 g, 1.0 mmol) was added to cause an immediate color change from red to dark red. After stirring for 6 h, volatiles were removed under vacuum. The residue was washed by *n*-hexane (20 mL) and reacted with H_2SO_4 (1.0 mL, 18 mmol) in CH_2Cl_2 (20 mL) at room temperature. The resulting solution was stirred for 20 h, and then H_2O (25 mL) was added. The organic phase was collected, the volatiles were removed, and the residue was subjected to TLC using CH_2Cl_2 /petroleum ether ($v/v = 1:4$) as eluent. From the main red band, 10 (0.176 g, 26%) was obtained as a red solid. Anal. calcd for $\text{C}_{25}\text{H}_{16}\text{F}_3\text{Fe}_2\text{O}_6\text{PS}_2$: C, 44.41; H, 2.39. Found: C, 44.25; H, 2.61. IR (KBr disk): $\nu_{\text{C}=\text{O}}$ 2052 (s), 1987 (vs), 1940 (s) cm^{-1} . ^1H NMR (δ , ppm, 500 MHz, CDCl_3): 7.13–7.7 (12H, 3C₆H₄), 3.76 (d, 2H, $2\text{OCH}_2\text{H}_e\text{S}$), 3.57 (d, 2H, $2\text{OCH}_2\text{H}_e\text{S}$). ^{13}C NMR (δ , ppm, 126 MHz, TMS): 67.66 (OCH₂S), 116.2, 132.02, 132.35, 135.52, 163.09, 165.12 (PhCH), 208.9 (s, FeCO), 213.52 (d, $^2J_{\text{PC}} = 10.1$ Hz, PFeCO). ^{31}P NMR (200 MHz, CDCl_3 , 85% H_3PO_4): 61.83 (s).

Synthesis of Complex $\text{Fe}_2[(\mu\text{-SCH}_2)_2\text{O}](\text{CO})_5[\text{P}(\text{C}_6\text{H}_4\text{-4-CH}_3)_3]$ (11). Complex 11 was synthesized in a fashion similar to that of complex 10 using $\text{P}(\text{C}_6\text{H}_4\text{-4-CH}_3)_3$ as the phosphine ligand. Yield: 25%, red solid. Anal. calcd for $\text{C}_{28}\text{H}_{23}\text{Fe}_2\text{O}_6\text{PS}_2$: C, 50.63; H, 3.79. Found: C, 50.55; H, 4.01. IR (KBr disk): $\nu_{\text{C}=\text{O}}$ 2049 (vs), 1988 (vs), 1971 (vs); 1935 (s) cm^{-1} . ^1H NMR (δ , ppm, 500 MHz, CDCl_3): 7.61, 7.24 (2s, 12H, $3\text{C}_6\text{H}_4$), 3.79 (s, 2H, $2\text{OCH}_2\text{H}_e\text{S}$), 3.44 (s, 2H, $2\text{OCH}_2\text{H}_e\text{S}$), 2.41 (s, 9H, 3CH_3). ^{13}C NMR (δ , ppm, 126 MHz, TMS): 21.54 (CH_3), 67.08 (OCH_2S), 129.33, 133.54, 140.48 (PhCH), 209.57 (s, FeCO), 213.82 (d, $^2J_{\text{PC}} = 10.0$ Hz, PFeCO). ^{31}P NMR (200 MHz, CDCl_3 , 85% H_3PO_4): 61.23 (s).

Synthesis of Complex $\text{Fe}_2[(\mu\text{-SCH}_2)_2\text{O}](\text{CO})_5[\text{PPh}_2(\text{CH}_2\text{CH}_3)]$ (12). Complex 12 was synthesized in a fashion similar to that of complex 10 using $\text{PPh}_2(\text{CH}_2\text{CH}_3)$ as the phosphine ligand. Yield: 22%, red solid. Anal. calcd for $\text{C}_{21}\text{H}_{19}\text{Fe}_2\text{O}_6\text{PS}_2$: C, 43.93; H, 3.34. Found: C, 43.83; H, 3.45. IR (KBr disk): $\nu_{\text{C}=\text{O}}$ 2046 (vs), 1981 (vs), 1929 (s) cm^{-1} . ^1H NMR (δ , ppm, 500 MHz, CDCl_3): 7.71, 7.43 (2s, 10H, $2\text{C}_6\text{H}_5$), 3.72 (s, 4H, $2\text{OCH}_2\text{S}$), 2.50–2.53 (m, 2H, CH_2), 1.16–1.23 (m, 3H, CH_3). ^{13}C NMR (δ , ppm, 126 MHz, TMS): 8.69 (CH_3), 27.06 (CH_2), 67.85 (OCH_2S), 128.56, 128.63, 130.18, 132.66 (PhCH), 209.35 (s, FeCO), 214.54 (d, $^2J_{\text{PC}} = 10.0$ Hz, PFeCO). ^{31}P NMR (200 MHz, CDCl_3 , 85% H_3PO_4): 57.56 (s).

CONCLUSION

In summary, we report on the synthesis of nine new phosphine-substituted diiron azadithiolate complexes and three new phosphine-substituted diiron oxadithiolate complexes via an interesting one-pot reaction. Reaction of $\text{Fe}_2(\mu\text{-SCH}_2\text{OH})_2(\text{CO})_6$ and several phosphine ligands L (L = PPh_3 , $\text{PPh}_2(2\text{-C}_5\text{H}_4\text{N})$, $\text{P}(\text{C}_6\text{H}_4\text{-4-CH}_3)_3$) affords the intermediate $\text{Fe}_2(\mu\text{-SCH}_2\text{OH})_2(\text{CO})_5\text{L}$, while the intermediate *in situ* reacts with primary amines RNH_2 (R = $\text{CH}_2\text{CH}_2\text{CH}(\text{CH}_3)_2$, $\text{CH}_2\text{CH}_2\text{CH}_2\text{SCH}_3$, $\text{C}_6\text{H}_4\text{-4-CH}_3$) to produce the target phosphine-substituted diiron azadithiolate complexes $\text{Fe}_2[(\mu\text{-SCH}_2)_2\text{NR}](\text{CO})_5\text{L}$ in moderate yields. Comparatively, the traditional way to synthesize this kind of the diiron azadithiolate complexes with monophosphine ligands needs two steps. The first step is to synthesize the all-carbonyl diiron azadithiolate complexes $\text{Fe}_2[(\mu\text{-SCH}_2)_2\text{NR}](\text{CO})_6$. The second step is further treatment of the as-prepared complexes $\text{Fe}_2[(\mu\text{-SCH}_2)_2\text{NR}](\text{CO})_6$ with phosphine ligand in the presence of decarbonylating agent Me_3NO affords the target phosphine-substituted complexes $\text{Fe}_2[(\mu\text{-SCH}_2)_2\text{NR}](\text{CO})_5\text{L}$. Compared with the widely used traditional way, this novel one-pot method is simpler and more efficient. In this paper, a series of new phosphine-substituted diiron azadithiolate complexes 1–8 have been successfully synthesized by the one-pot reaction in satisfactory yield. In addition, reaction of $\text{Fe}_2(\mu\text{-SCH}_2\text{OH})_2(\text{CO})_6$ and $\text{Ph}_2\text{PCH}_2\text{CH}_2\text{NH}_2$ affords complex $\text{Fe}_2[(\mu\text{-SCH}_2)_2\text{NCH}_2\text{CH}_2\text{PPh}_2](\text{CO})_5$ (9). In addition, according to the same strategy, phosphine-substituted diiron oxadithiolate complexes $\text{Fe}_2[(\mu\text{-SCH}_2)_2\text{O}](\text{CO})_5[\text{P}(\text{C}_6\text{H}_4\text{-4-F})_3]$ (10), $\text{Fe}_2[(\mu\text{-SCH}_2)_2\text{O}](\text{CO})_5[\text{P}(\text{C}_6\text{H}_4\text{-4-CH}_3)_3]$ (11), and $\text{Fe}_2[(\mu\text{-SCH}_2)_2\text{O}](\text{CO})_5(\text{Ph}_2\text{PCH}_2\text{CH}_3)$ (12) have been successfully synthesized. All of the new complexes 1–12 were fully characterized by elemental analysis, IR, and NMR spectroscopy, and particularly for 1–4, 6, 7, and 9–11 by X-ray single diffraction analysis. Moreover, the electrochemical properties of complexes 1–6 and 10 were investigated by CV in DCM solution. Complexes 1 and 10 were found to be catalysts for H_2 production under electrochemical conditions. Further study on the synthesis of diiron azadithiolate complexes containing different diphosphine ligands is in progress in our research group.

ASSOCIATED CONTENT

Supporting Information

The Supporting Information is available free of charge on the ACS Publications website at DOI: 10.1021/acs.organomet.7b00040.

CV curves for 1–6, IR and NMR spectra for 1–12 (PDF)

Crystallographic data for 1–4, 6, 7, and 9–11 (CIF)

AUTHOR INFORMATION

Corresponding Authors

*E-mail: yu_longli@aliyun.com.

*E-mail: zph2004@nuc.edu.cn.

Notes

The authors declare no competing financial interest.

ACKNOWLEDGMENTS

Financial support for this work was provided by National Natural Science Foundation of China (21501124, 21301160), Science & Technology Department of Sichuan Province (2017JY0195, 2016086), Zigong Science & Technology and Intellectual Property Bureau (2014HX02, 2015CXM01), Sichuan University of Science & Engineering (2014RC05), and Material Corrosion and Protection of Key Laboratory of Sichuan Province (2014CL14).

REFERENCES

- (1) Adams, M. W. W. *Biochim. Biophys. Acta, Bioenerg.* **1990**, *1020*, 115–145.
- (2) Evans, D. J.; Pickett, C. J. *Chem. Soc. Rev.* **2003**, *32*, 268–275.
- (3) Volbeda, A.; Fontecilla-Camps, J. C. *Coord. Chem. Rev.* **2005**, *249*, 1609–1619.
- (4) Fontecilla-Camps, J. C.; Volbeda, A.; Cavazza, C.; Nicolet, Y. *Chem. Rev.* **2007**, *107*, 4273–4303.
- (5) Lubitz, W.; Ogata, H.; Rüdiger, O.; Reijerse, E. *Chem. Rev.* **2014**, *114*, 4081–4148.
- (6) (a) Wenk, S. O.; Qian, D. J.; Wakayama, T.; Nakamura, C.; Zorin, N.; Rögner, M.; Miyake, J. *Int. J. Hydrogen Energy* **2002**, *27*, 1489–1493. (b) Chu, X.-X.; Xu, X.; Su, H.; Rajee, S.; Angamuthu, R.; Tung, C.-H.; Wang, W.-G. *Inorg. Chem. Front.* **2017**, DOI: 10.1039/C6QJ00536E. (c) Zhang, F.-J.; Jia, J.; Dong, S.-L.; Wang, W.-G.; Tung, C.-H. *Organometallics* **2016**, *35*, 1151–1159.
- (7) (a) Peters, J. W.; Lanzilotta, W. N.; Lemon, B. J.; Seefeldt, L. C. *Science* **1998**, *282*, 1853–1858. (b) Nicolet, Y.; Piras, C.; Legrand, P.; Hatchikian, C. E.; Fontecilla-Camps, J. C. *Structure* **1999**, *7*, 13–23. (c) Lemon, B. J.; Peters, J. W. *Biochemistry* **1999**, *38*, 12969–12973.
- (8) Pandey, A. S.; Harris, T. V.; Giles, L. J.; Peters, J. W.; Szilagyi, R. K. *J. Am. Chem. Soc.* **2008**, *130*, 4533–4540.
- (9) Nicolet, Y.; de Lacey, A. L.; Vernède, X.; Fernandez, V. M.; Hatchikian, E. C.; Fontecilla-Camps, J. C. *J. Am. Chem. Soc.* **2001**, *123*, 1596–1601.
- (10) Li, H.-X.; Rauchfuss, T. B. *J. Am. Chem. Soc.* **2002**, *124*, 726–727.
- (11) Berggren, G.; Adamska, A.; Lambert, C.; Simmons, T. R.; Esselborn, J.; Atta, M.; Gambarelli, S.; Mouesca, J. M.; Reijerse, E.; Lubitz, W.; Happe, T.; Artero, V.; Fontecave, M. *Nature* **2013**, *499*, 66–69.
- (12) Bethel, R. D.; Darensbourg, M. Y. *Nature* **2013**, *499*, 40–41.
- (13) (a) Gilbert-Wilson, R.; Siebel, J. F.; Adamska-Venkatesh, A.; Pham, C. C.; Reijerse, E.; Wang, H.; Cramer, S. P.; Lubitz, W.; Rauchfuss, T. B. *J. Am. Chem. Soc.* **2015**, *137*, 8998–9005. (b) Xu, J.-H.; Guo, L.-Y.; Su, H.-F.; Gao, X.; Wu, X.-F.; Wang, W.-G.; Tung, C.-H.; Sun, D. *Inorg. Chem.* **2017**, *56*, 1591–1598. (c) Jian, J.-X.; Liu, Q.; Li, Z.-J.; Wang, F.; Li, X.-B.; Li, C.-B.; Liu, B.; Meng, Q.-Y.; Chen, B.; Feng, K.; Tung, C.-H.; Wu, L.-Z. *Nat. Commun.* **2013**, *4*, 3695.

- (14) Li, Y.-L.; Rauchfuss, T. B. *Chem. Rev.* **2016**, *116*, 7043–7077.
- (15) Stanley, J. L.; Rauchfuss, T. B.; Wilson, S. R. *Organometallics* **2007**, *26*, 1907–1911.
- (16) Jiang, S.; Liu, J.; Shi, Y.; Wang, Z.; Åkermark, B.; Sun, L.-C. *Dalton Trans.* **2007**, 896–902.
- (17) Angamuthu, R.; Chen, C.-S.; Cochrane, T. R.; Gray, D. L.; Schilter, D.; Ulloa, O. A.; Rauchfuss, T. B. *Inorg. Chem.* **2015**, *54*, 5717–5724.
- (18) Singleton, M. L.; Reibenspies, J. H.; Darensbourg, M. Y. *J. Am. Chem. Soc.* **2010**, *132*, 8870–8871.
- (19) Gao, W.-M.; Sun, J.-L.; Åkermark, T.; Li, M.-R.; Eriksson, L.; Sun, L.-C.; Åkermark, B. *Chem. - Eur. J.* **2010**, *16*, 2537–2546.
- (20) Esmieu, C.; Berggren, G. *Dalton Trans.* **2016**, *45*, 19242–19248.
- (21) Jiang, S.; Liu, J.-H.; Sun, L.-C. *Inorg. Chem. Commun.* **2006**, *9*, 290–292.
- (22) Song, L.-C.; Yin, B.-S.; Li, Y.-L.; Zhao, L.-Q.; Ge, J.-H.; Yang, Z.-Y.; Hu, Q.-M. *Organometallics* **2007**, *26*, 4921–4929.
- (23) Song, L.-C.; Tang, M.-Y.; Su, F.-H.; Hu, Q.-M. *Angew. Chem., Int. Ed.* **2006**, *45*, 1130–1133.
- (24) Rauchfuss, T. B. *Acc. Chem. Res.* **2015**, *48*, 2107–2116.
- (25) Liu, T.-B.; Wang, M.; Shi, Z.; Cui, H.-G.; Dong, W. B.; Chen, J.-S.; Åkermark, B.; Sun, L.-C. *Chem. - Eur. J.* **2004**, *10*, 4474–4479.
- (26) Tard, C.; Pickett, C. J. *Chem. Rev.* **2009**, *109*, 2245–2274.
- (27) Si, G.; Wang, W.-G.; Wang, H.-Y.; Tung, C.-H.; Wu, L.-Z. *Inorg. Chem.* **2008**, *47*, 8101–8111.
- (28) Wang, W.-G.; Wang, H.-Y.; Si, G.; Tung, C.-H.; Wu, L.-Z. *Dalton Trans.* **2009**, *15*, 2712–2720.
- (29) Gloaguen, F.; Lawrence, J. D.; Schmidt, M.; Wilson, S. R.; Rauchfuss, T. B. *J. Am. Chem. Soc.* **2001**, *123*, 12518–12527.
- (30) Zhao, X.; Chiang, C.-Y.; Miller, M. L.; Rampersad, M. V.; Darensbourg, M. Y. *J. Am. Chem. Soc.* **2003**, *125*, 518–524.
- (31) Liu, T.-B.; Darensbourg, M. Y. *J. Am. Chem. Soc.* **2007**, *129*, 7008–7009.
- (32) Song, L.-C.; Yang, Z.-Y.; Bian, H.-Z.; Liu, Y.; Wang, H.-T.; Liu, X.-F.; Hu, Q.-M. *Organometallics* **2005**, *24*, 6126–6135.
- (33) Lawrence, J. D.; Li, H.-X.; Rauchfuss, T. B. *Chem. Commun.* **2001**, 1482–1483.
- (34) Ott, S.; Borgstrom, M.; Kritikos, M.; Lomoth, R.; Bergquist, J.; Åkermark, B.; Hammarstrom, L.; Sun, L.-C. *Inorg. Chem.* **2004**, *43*, 4683–4692.
- (35) Wang, Z.; Liu, J.-H.; He, C.-J.; Jiang, S.; Åkermark, B.; Sun, L.-C. *J. Organomet. Chem.* **2007**, *692*, 5501–5507.
- (36) Li, Y.-L.; Xie, B.; Zou, L.-K.; Zhang, X.-L.; Lin, X. J. *Organomet. Chem.* **2012**, *718*, 74–77.
- (37) Capon, J. F.; Ezzaher, S.; Gloaguen, F.; Petillon, F. Y.; Schollhammer, P.; Talarmin, J.; Davin, T. J.; McGrady, J. E.; Muir, K. W. *New J. Chem.* **2007**, *31*, 2052–2064.
- (38) Song, L.-C.; Xie, Z.-J.; Liu, X.-F.; Ming, J.-B.; Ge, J.-H.; Zhang, X.-G.; Yan, T.-Y.; Gao, P. *Dalton Trans.* **2011**, *40*, 837–846.
- (39) Si, Y.-T.; Ma, C.-B.; Hu, M.-Q.; Chen, H.; Chen, C.-N.; Liu, Q.-T. *New J. Chem.* **2007**, *31*, 1448–1454.
- (40) Singleton, M. L.; Crouthers, D. J.; Duttweiler, R. P.; Reibenspies, J. H.; Darensbourg, M. Y. *Inorg. Chem.* **2011**, *50*, 5015–5026.
- (41) Song, L.-C.; Cao, M.; Du, Z.-Q.; Feng, Z.-H.; Ma, Z.; Song, H.-B. *Eur. J. Inorg. Chem.* **2014**, *2014*, 1886–1895.
- (42) Borg, S. J.; Behrsing, T.; Best, S. P.; Razavet, M.; Liu, X. M.; Pickett, C. J. *J. Am. Chem. Soc.* **2004**, *126*, 16988–16999.
- (43) Capon, J.-F.; Ezzaher, S.; Gloaguen, F.; Pétillon, P. S.; Talarmin, J. *Chem. - Eur. J.* **2008**, *14*, 1954–1964.
- (44) Vannucci, A. K.; Wang, S.; Nichol, G. S.; Lichtenberger, D. L.; Evans, D. H.; Glass, R. S. *Dalton Trans.* **2010**, *39*, 3050–3056.
- (45) Seyferth, D.; Henderson, R. S.; Song, L.-C. *Organometallics* **1982**, *1*, 125–133.
- (46) Sheldrick, G. M. *SHELXS97, A Program for Crystal Structure Solution*; University of Göttingen: Göttingen, Germany, 1997.
- (47) Sheldrick, G. M. *SHELXL97, A Program for Crystal Structure Refinement*; University of Göttingen: Göttingen, Germany, 1997.